COMPACT INFRARED SOURCES:

NGC 7538 AND THE GALACTIC CENTER

Thesis by

Steven Paul Willner

In Partial Fulfillment of the Requirements

for the Degree of

Doctor of Philosophy

California Institute of Technology

Pasadena, California

1976

(Submitted 1976 January 29)

ACKNOWLEDGEMENTS

I wish to thank E. E. Becklin and G. Neugebauer for their advice, encouragement, help, and criticism. The map and broadband photometry reported in Chapter 2 were done jointly with them during their observing time.

I thank the Director of the Hale Observatories for a generous allotment of observing time, G. W. Preston for scheduling the time most conveniently, the night assistants E. Hancock, H. Lanning, M. Marcario, and G. Tuton, and C. Bornhurst and E. Lorenz of the Mt. Wilson Observatory for their help and cooperation. I am also grateful to the many people who assisted in obtaining the observations; those who did so most often were S. Beckwith, T. A. Boroson, N. G. Brown, J. Elias, and J. P. Huchra.

I have enjoyed valuable discussions with a great many people; among them are J. A. Frogel, I. Gatley, K. Matthews, and J. A. Westphal. I especially thank J. A. W. for his patience and understanding in a moment of stress.

I received financial support from Graduate Research Assistantships and a National Science Foundation Fellowship. Support for my research came from National Aeronautics and Space Administration grant NGL 05-002-207 and National Science Foundation grant MPS74-18555A01, which support infrared astronomy at Caltech.

Finally, I thank S. Hage and T. Smith for their rapid and accurate typing of various drafts and the final version of this thesis. I am especially grateful to S. H. for typing during a weekend in order to meet a deadline.

ABSTRACT

Three infrared and radio sources in NGC 7538 have been observed from 8 to 13 μ with 1% spectral and 5" spatial resolution. The very small southern source shows a deep silicate absorption feature at 9.7 μ while the northern extended source shows little or no silicate absorption, but has a 12.8-μ emission line from Ne II. The data imply that the compact source has a gas to dust ratio of 75 inside the ionized region. The extended source only 10" away has a gas to dust ratio implied by the 10-μ data alone of 3×10^4, but the true ratio must be much lower to account for published 20-μ measurements.

A revised 10-μ map of the Galactic center with 2".3 resolution, broadband photometry of individual sources from 1.2 to 20 μ, and 8 to 13-μ photometry of individual sources with 1% spectral resolution have been obtained. The principal conclusions of this study are: (1) The five sources with the bluest energy distributions between 1.6 and 3.5 μ are stars or star clusters. The brightest has a luminosity of 10^5 $L_\odot$ while the other four have luminosities of about 10^4 $L_\odot$. (2) There is extended emission from ionized gas and dust. (3) The density of ionized gas in the discrete 10-μ sources is no higher than that in the extended source. (4) There is at least one compact source that is not associated with the others and has a different energy distribution. (5) Most of the extinction toward the sources observed is interstellar and is moderately uniform. The visual extinction is about 28 magnitudes, and the 9.7-μ silicate extinction is about 3.7 magnitudes.

TABLE OF CONTENTS

	Page
ACKNOWLEDGEMENTS	ii
ABSTRACT	iii
TABLE OF CONTENTS	iv
LIST OF TABLES	vi
LIST OF FIGURES	vii
INTRODUCTION	viii
CHAPTER 1: NGC 7538	xii
I. Introduction	1
II. Observations	2
III. Emission Lines	6
IV. The Silicate Feature	8
V. Conclusion	18
Appendix	19
References	21
CHAPTER 2: THE GALACTIC CENTER	23
I. Introduction	24
II. Observations	25
III. Discussion	31
a) Extinction at Short Wavelengths	31
b) Silicate Extinction	34
c) IRS7	41
d) Stellar Sources - IRS11, 12, 16, and 19	44
e) Ridge Sources - IRS1, 2, 5, 6, 9, and 10	44

CHAPTER 2 (Continued)

f) Other Sources - IRS3 and 8 52

g) Extended Emission - IRS4 52

IV. Conclusions 54

References 55

LIST OF TABLES

Page

CHAPTER 1:

1. Possible Emission Lines in IRS2 7
2. Neon Abundance 9
3. Best Fit Model Parameters 11
4. Cloud Masses and Gas to Dust Ratios 14

CHAPTER 2:

1. Observations and Adopted Extinction Corrections 28
2. Relative Silicate Optical Depth 35
3. Absorption at 9.7 μ 36
4. Ne II Observations 46

LIST OF FIGURES

Page

CHAPTER 1:

1. 8- to 13-μ Spectra of IRS1 4

2. 8- to 13-μ Spectra of IRS2 and IRS3 5

CHAPTER 2:

1. Map of the Galactic Center Region at 10 μ 26

2. The Positions and Size of the 5" Spectrometer Aperture Superposed on the 10-μ Map 29

3. Observed Fluxes from 7.5 to 13.5 μ 30

4. Corrected Energy Distributions of Four Sources with no 10-μ Counterparts 33

5. Energy Distribution of IRS7 Corrected for Extinction 42

6. Energy Distributions Corrected for Extinction of Four Sources 49

7. 8- to 13-μ Energy Distributions Corrected for Extinction of all Ten 10-μ Sources Observed 50

INTRODUCTION

This thesis consists of two separate papers. They have in common a presentation of detailed studies of individual sources in regions where maps have shown many sources in a small area. The motivation for these studies was that by studying sources in a cluster, one might begin to understand what properties are characteristic of individual sources and what properties apply to the whole cluster.

The two papers also have in common that much of the observing was done with the same instrument--an 8 to 13 micron spectrometer. The major characteristics of the instrument are described in Chapter 1. A large portion of my career as a graduate student was devoted to building, testing, and repairing this instrument, and some details of it are presented here.

The spectrometer is built inside a liquid helium dewar designed by J. A. Westphal. Light from a telescope or test source is admitted through a barium fluoride window, passes through a filter, an aperture, and a field lens and lands on the detector. The filter can be any of up to four broadband filters or can be a circular variable filter (CVF) for high resolution observations. The CVF is in the form of a half disk and is mounted so that as it rotates the light path passes through different azimuths of the CVF; each azimuth transmits a different wavelength. As the filter mounting is rotated further, the CVF passes out of the light path and the broadband filters are brought into it.

The rotation of the CVF is accomplished manually through a system of gears and a shaft passing through an airtight seal to the outside of the dewar. An external counter keeps track of the position of the shaft, and a set of detents are provided so that settings may be easily reproduced. Because the measurement of the position of the CVF is tied to the CVF itself only through a system of gears, these gears and all couplings must be carefully adjusted to minimize backlash and slippage. In practice it was found that slippage was nonexistent, while backlash amounted to 0.2 to 0.3 of a resolution element. Because of the backlash, all of the spectra were measured with the CVF having last been turned toward increasing wavelength; the backlash was then negligible.

The detents are approximately one resolution element apart; for the highest spectral resolution possible with this instrument it would have been necessary to use twice as many detents. This was not considered justified in view of the observing time that would have been required to measure so many points. Even with the present spacing, it was often possible to measure only one-half or one-fourth of the usual number of points on the faintest objects.

The first step in the usual observing procedure was to center the object in the aperture by maximizing the signal through a broadband filter. An offset guider was then centered on a visible star, and the spectrum was measured as described in Chapter 1. The broadband filter was put back in and the centering of the object checked as often as was necessary to compensate for differential refraction

between the infrared light being measured and the visible light from the star used for guiding.

The use of standards is described in Chapter 1. Both a relative standard, to give the instrumental sensitivity as a function of wavelength, and an absolute standard, to give the absolute sensitivity at one wavelength, were needed. The Moon was used as the primary relative standard because it was found that measurements of it were reproducible to within 2 to 3%, while measurements of stars were reproducible only to within 5 to 7%. The extra error in measurements of stars was probably due to guiding errors, because part of the flux from the stars fell outside the small apertures used and because the wavelength changed as the position of the star in the aperture changed. Stars were used as absolute standards, and were also used to determine that the bright limb of the Moon radiates as a grey body at a temperature of 350 K at wavelengths between 8 and 13 μ.

Observations with a spectrometer have two advantages over observations with intermediate bandwidth filters. The first is that the spectrometer can detect and measure emission lines. Secondly, the spectrometer can measure the shape of broad features such as the silicate absorption. The shape observed in one object can be compared to that observed in others as well as to laboratory measurements; the comparisons may lead to identification of the feature. Intermediate bandwidth observations are excellent for comparing the strength of a feature in different objects, but are meaningful only if it is known or assumed that the same feature is being measured in all cases. Both

narrow and intermediate bandwidth observations are presented in Chapter 2, where they can be compared.

CHAPTER 1

NGC 7538

I. INTRODUCTION

The large optically visible H II region NGC 7538 contains three compact radio and infrared sources in an area 24" by 24". This area has been mapped at 5 GHz by Martin (1973) and at 2.2 and 20 μ by Wynn-Williams, Becklin, and Neugebauer (1974 - hereafter WBN). Both the radio and infrared maps show three sources: IRS 1, 1".5 in diameter, which is bright in the infrared but faint in the radio; IRS 2, 9" in diameter, which is bright in the radio but fainter than IRS 1 at 10 μ; and IRS 3, 2".7 in diameter, which has an energy distribution intermediate between those of IRS 1 and IRS 2 but is fainter than both at all wavelengths. Martin (1973) estimated upper limits for the ages of the compact sources of 4000 to 25,000 years from the radii of the H II regions and the speed of sound in ionized gas. An OH maser is associated with IRS 1 (Wynn-Williams, Werner, and Wilson 1974), and molecular emission from CO is found over a region nearly a degree in diameter (Wilson et al. 1974). Emission lines from H_2S (Thaddeus et al. 1972), CS (Turner et al. 1973), HCN (Morris et al. 1974), and H_2CO (Downes and Wilson 1974) have been detected from the area of the compact infrared and radio sources, and the brightest CO emission peak is at that position (Wilson et al. 1974).

Broadband infrared measurements have shown that IRS 1 has a silicate absorption feature near 10 μ, while IRS 2 does not (WBN). Aitken, Jones, and Penman (1974) have obtained 8 to 13-μ spectra of several H II regions including NGC 7538. Their field of view included both IRS 1 and IRS 2 and showed a deep silicate absorption feature at wavelengths near 10 μ. Spectra of compact sources in other H II regions have been obtained by Gillett et al. (1975a) (hereafter GFMCS). These spectra

showed a silicate absorption feature and often an emission line of Ne II at 12.8 μ. The Ne line flux generally indicated a Ne II abundance below the cosmic abundance of neon.

In this paper, observations which spatially separate the three compact sources with spectral resolution $\Delta\lambda/\lambda = 0.01$ from $\lambda = 7.4$ to 13.5 μ are presented. The instrument and observing techniques are described in § II. § III describes observations of emission lines in IRS 2. Models are fitted to the observed emission in § IV, various source parameters are derived, and the masses of the compact H II regions and their gas to dust ratios are estimated and interpreted. An estimate is also made of the mass of the material shown to be present around IRS 1. § V summarizes the results.

II. OBSERVATIONS

The spectrometer uses a liquid nitrogen cooled circular variable filter as the wavelength selective element. A barium fluoride Fabry lens images the primary of the telescope onto an arsenic-doped silicon detector, which is cooled with liquid helium. Observations are made by setting the wavelength, integrating using normal infrared chopping and beam switching techniques, and advancing to the next wavelength. The wavelengths measured are separated by 0.117 μ, which is slightly larger than the spectral resolution of 1% of the wavelength over most of the spectral range.

Normally measurements are made at every second wavelength step, then the filter is returned to the start, and measurements are made at the wavelengths which were skipped the first time. This procedure acts as a check on possible systematic errors due to guiding, changing atmospheric extinction, or changing instrumental sensitivity.

Most of the observations reported here were made on 1974 August 31 to September 4 and November 11 and 14 with the 100-inch Hooker telescope. The August/September observations used a 5" aperture and a 20" beam separation in declination while the November observations used a 7".5 aperture and a 17".5 separation in declination. The flux of IRS 1 was independent of aperture so all the measurements of it were averaged. The flux of IRS 2 increased by 0.39 ± .05 magnitudes with the larger aperture; the observations of it were corrected to a 5" aperture before averaging. IRS 3 was observed only with the 5" aperture. The results are shown in Figures 1 and 2.

The instrumental sensitivity as a function of wavelength was determined by measuring standard stars and the limb of the moon. The moon was assumed to radiate as a 350 K blackbody, which was found to be consistent with the hot stars having a Rayleigh-Jeans spectrum. An attempt was made to observe the standards and the objects at the same air mass, and residual differences in atmospheric extinction were compensated for in the data reduction using absorption parameters from Goldman (1970) for ozone and from McClatchey et al. (1972) for other gases. Absolute calibration was provided by observing α Tauri and assuming its flux at 10.1 μ is 1.91×10^{-15} W cm^{-2} μ^{-1}, consistent

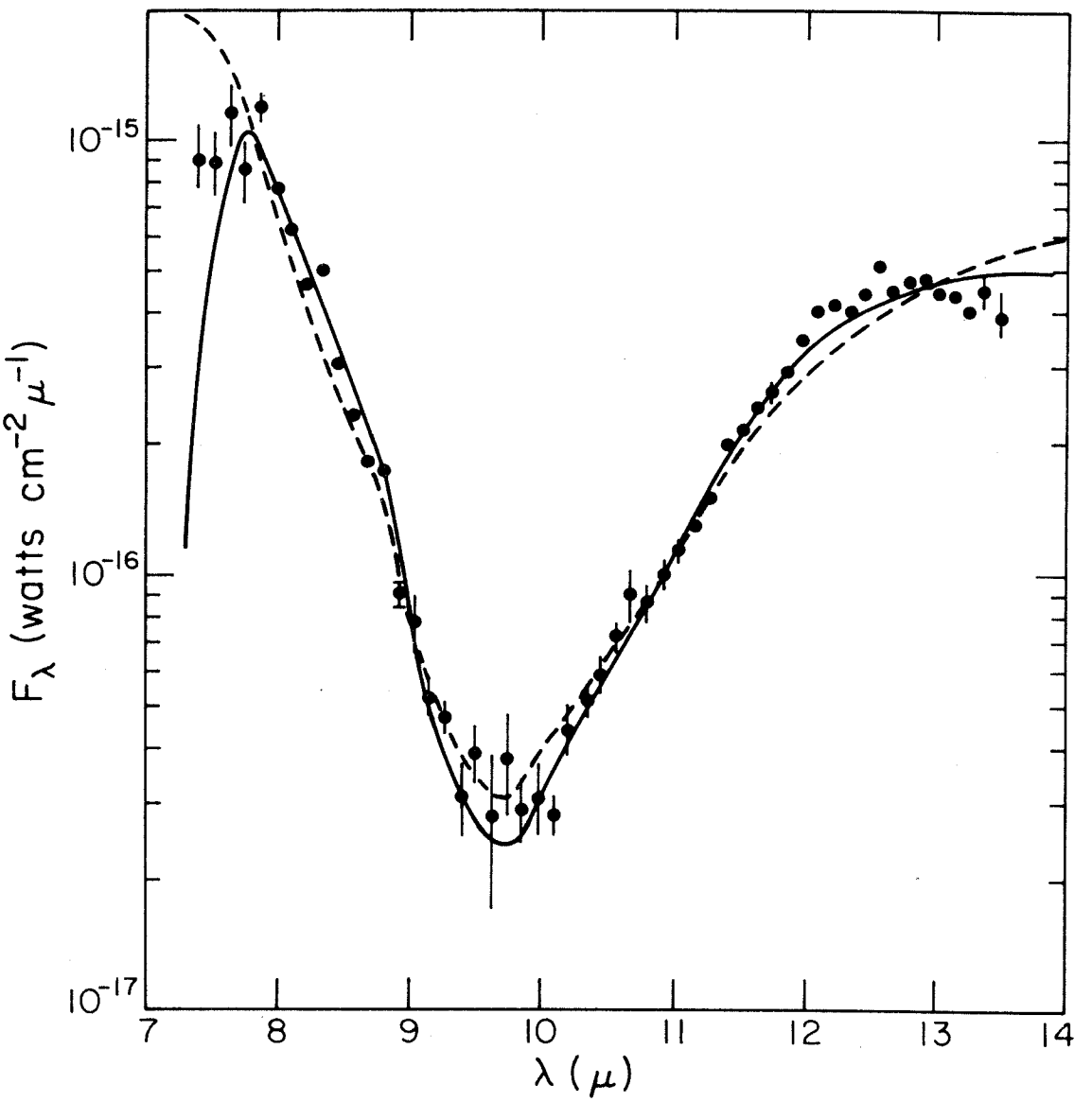

Figure 1

8- to 13-μ spectra of IRS1. Error bars are given for the points with larger errors than 5%. The solid line is the spectrum predicted by the model with Trapezium-like emissivity, and the dashed line is that for blackbody emissivity.

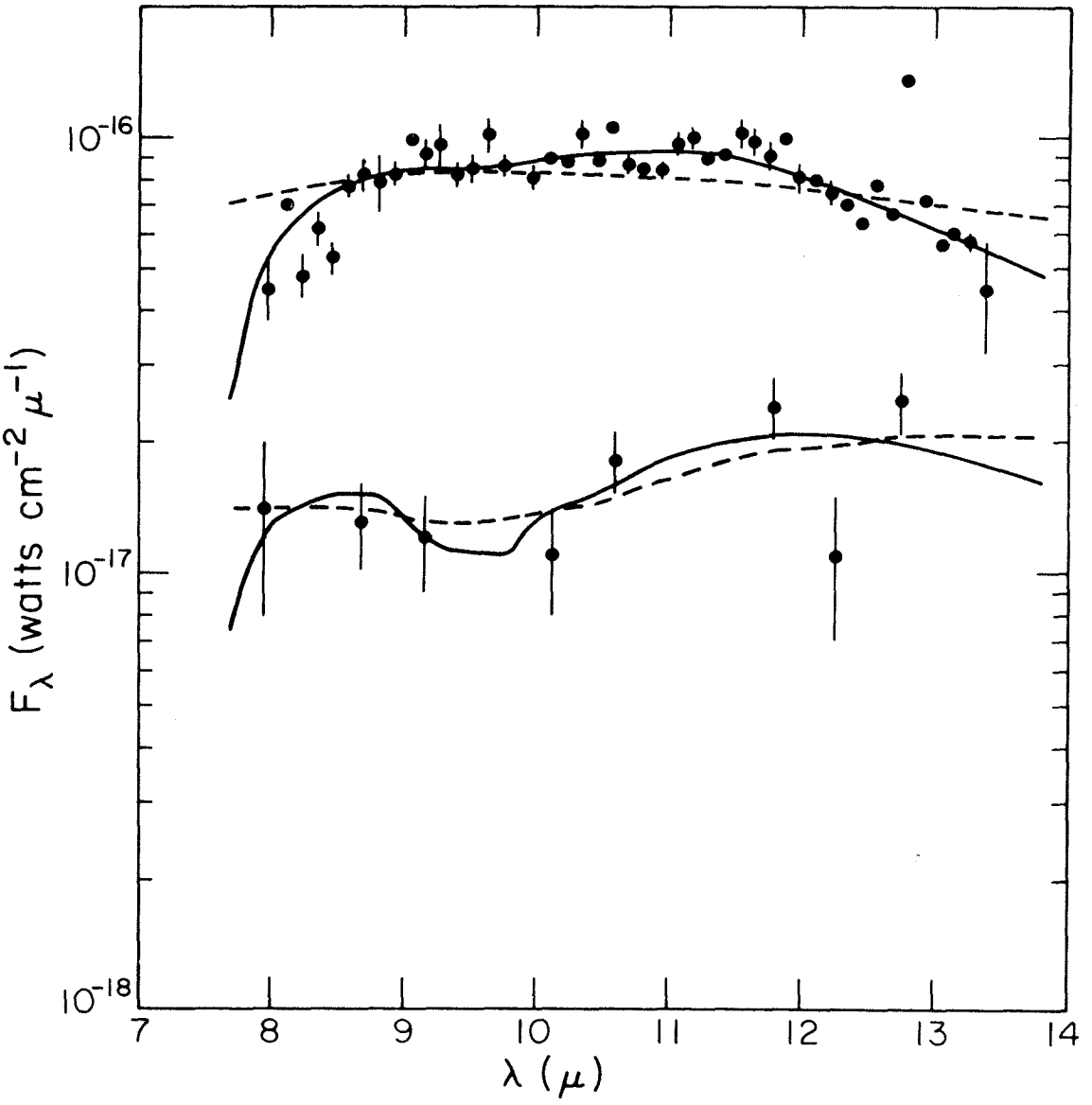

Figure 2

8- to 13-μ spectra of IRS2 (upper) and IRS3 (lower). See the caption for Figure 1.

with the Caltech broadband photometry.

In the spectra presented here, points near 12.8 μ, the wavelength of the Ne II line, were observed in succession in order to minimize systematic errors in measuring the line flux. These points were repeatedly measured on different nights as a further check on their accuracy. At other wavelengths, consecutive points were observed on different nights as a check on possible calibration errors.

Additional observations at wavelengths near 8.99 and 10.53 μ were obtained on 1975 June 20 and 21, in order to search for the predicted Ar III and S IV emission lines. The lines were not found, and the 3 σ upper limits are given in Table 1, along with the measurement of the Ne II line at 12.8 μ.

III. EMISSION LINES

The spectra presented in Figures 1 and 2 show that a strong Ne II line is present at 12.8 μ in IRS 2 but is absent in IRS 1. The nominal wavelengths, identifications, and the fluxes in this line and the upper limits on two other possible emission lines in IRS 2 are given in Table 1. The data for IRS 3 are insufficient to detect any emission lines.

The abundance of Ne II relative to H II for IRS 2 and an upper

TABLE 1

POSSIBLE EMISSION LINES IN IRS 2

λ	Identification	Measured Flux 10^{-18} W cm^{-2}	Corrected Flux 10^{-18} W cm^{-2}
9.04	Ar III λ 8.99	< 1.1	< 3.4
10.57	S IV λ 10.53	< 1.3	< 4.0
12.79	Ne II λ 12.78	9.0 ± .9	14

limit for IRS 1 can be derived using the formulation of Petrosian (1970); the results are given in Table 2. The 12.8-μ flux has been corrected for absorption by dust as discussed below. The neon abundance in IRS 2 is slightly below the cosmic abundance, but this is easily accounted for if some of the neon is doubly ionized, as suggested by GFMCS for other H II regions. Because the infrared continuum flux from IRS 1 is large compared to the radio flux, the measurements do not imply any difference in the Ne II abundance in the two sources.

IV. THE SILICATE FEATURE

The prominent absorption feature from 8 to 12 μ in IRS 1 shown in Figure 1 is of the same type as that identified as due to silicates in the Becklin-Neugebauer point source in the Orion Nebula, the Galactic center, and numerous sources in other H II regions (GFMCS and references therein). The feature in IRS 1 is one of the strongest such absorptions known, and indicates that a large amount of relatively cold dust lies along the line of sight to IRS 1. Because no feature of comparable strength is seen in IRS 2 or IRS 3, which are only 10" away, the cold dust must be directly associated with IRS 1.

The quantities which can be most directly derived from the observations are the mass of emitting dust, its temperature, and the column density of absorbing dust in front of IRS 1. These quantities were calculated assuming that the emitting dust particles are all at the same temperature and are in a separate region behind a layer of

TABLE 2

NEON ABUNDANCE

Object	Radio Flux* 10^{-26} Wm^{-2} Hz^{-1}	Measured 12.8-μ Flux 10^{-18} W cm^{-2}	Corrected 12.8-μ Flux 10^{-18} W m^{-2}	log[N(Ne II)/N(H II)]
IRS 1	0.12	< 4.4	< 30	< - 3.0
IRS 2	1.4	9.0 ± .9	14	- 4.4

*from Martin (1973)

absorbing silicate dust. The observed flux can then be fit to a function of wavelength λ of the form

$$F_\lambda = \Omega\, \epsilon(\lambda)\, B_\lambda\, (T_d)\, e^{-\tau(\lambda)}\ , \qquad (1)$$

where B_λ is the Planck function and ϵ is the emissivity. The absorption optical depth $\tau(\lambda)$ was assumed to be proportional to F_λ (Trap)/B_λ (T_T), where F_λ (Trap) is the flux from the Trapezium (Forrest, Gillett, and Stein 1975), and T_T is an assumed temperature of the Trapezium. The parameters derived from the model fit are the temperature T_d of the emitting dust, the peak optical depth $\tau(9.7)$ of the absorbing dust, and the effective solid angle Ω. Details of the model are in the Appendix.

The same two models for the emissivity $\epsilon(\lambda)$ of the hot dust were used as were used by GFMCS. The first model, that of Trapezium-like emission, sets $\epsilon(\lambda) \propto F_\lambda$ (Trap)/B_λ (T_T). The second model, that of blackbody emission, sets $\epsilon(\lambda) = 1$. Models such as $\epsilon(\lambda) \propto \lambda^{-1}$ or other smooth functions of wavelength generally give the same accuracy of fit to the observations as the blackbody emission model but with a different T_d.

The best fit model parameters are shown in Table 3. The calculated fluxes for Trapezium-like emissivity are shown as solid lines and for blackbody emissivity as dashed lines in Figures 1 and 2. The models do not seem to deviate from the observations in any systematic way, except that the very shortest wavelength observations of IRS 1 indicate an emissivity larger than that of the Trapezium. For all models the residuals from the model fit are larger than would be expected if only the observational statistical errors are considered. This is probably mostly due to the inaccuracy of the assumptions of a single temperature and Trapezium-like

TABLE 3

BEST FIT MODEL PARAMETERS

		Model with Trapezium-like Emissivity				Model with Blackbody Emissivity			
Object	N	Ω arc sec^2	T_d ^oK	$\tau(9.7)$	$\chi^2/N-3$	Ω arc sec^2	T_d ^oK	$\tau(9.7)$	$\chi^2/N-3$
IRS 1	53	2.6×10^{-1}	370 ± 40	6.4 ± 0.3	4.0	5.4×10^{-2}	330 ± 30	4.2 ± 0.2	9.0
IRS 2	46	2.7×10^{-2}	270 ± 20	1.4 ± 0.2	2.7	4.1×10^{-3}	290 ± 20	0	6.1
IRS 3	8	1.6×10^{-2}	250 ± 50	2.4 ± 0.8	1.8	3×10^{-3}	250 ± 50	0.6 ± 0.7	1.8

emissivity on which the models are based.

For both IRS 1 and IRS 2, Trapezium-like emissivity provides a much better fit to the data than blackbody emissivity; this conclusion is in agreement with that of GFMCS for other objects. In particular, for IRS 2, the best fit assuming blackbody emissivity had $\tau(9.7) = -0.4 \pm 0.2$, which is physically unreasonable. Therefore, all further discussions are based on Trapezium-like emissivity.

The visual extinctions to IRS 1, 2, and 3 can be crudely estimated from the depth of the silicate absorption. The extinctions are 90, 20, and 34 magnitudes repectively, if $A_V/\tau(9.7) = 14$ (Gillett et al. 1975b). These are consistent with IRS 1 and 3 being invisible on the Palomar sky survey red plates. A nebulosity does appear at the position of IRS 2 (WBN); the radio observations (Martin 1973) imply that the Hα surface brightness should be 13 mag $('')^{-2}$ and thus $A_{H\alpha} < 8$ and $A_V < 11$ mag. One explanation for the discrepancy between the low values of A_V implied by the short wavelength observations and the value of 20 mag implied by the 10-μ observations is that the dust is distributed non-uniformly in front of IRS 2, so that some parts of the nebula are heavily extinguished while other parts are extinguished hardly at all. Persson and Frogel (1974) have suggested that this is the case in K3-50, which also has a large silicate absorption but comparatively small visual extinction.

The mass of emitting dust in the H II regions can be obtained from

the models described above if the emission is optically thin, because the effective solid angle is directly proportional to the mass of emitting dust and its opacity per unit mass and inversely proportional to the square of the distance. That the emission is optically thin is shown in Table 4 which gives the emission optical depth $\tau_{em}(9.7)$ calculated from the effective solid angles derived from the model fits and from the radio diameters $\theta_{H\ II}$ of Martin (1973). The values of the mass of emitting dust M_d are also given in Table 4; the dust absorption coefficient $K(9.7)$ has been taken as 3×10^3 cm^2 g^{-1} (Gillett and Forrest 1973) and the distance as 3.5 kpc (Israel et al. 1973). The values of M_{gas}, the mass of ionized gas, are from Martin (1973), scaled to a distance of 3.5 kpc, and reduced by 40% in IRS 2 to allow for the small aperture. Table 4 also gives the calculated gas to dust ratios for the H II regions, assuming the infrared emission comes from the same region.

The gas to dust ratios of 3×10^4 and 10^3 indicated by the 10-μ data for the ionized regions of IRS 2 and IRS 3 are larger than the accepted interstellar value of 100 but comparable to the values found by GFMCS for other H II regions. These values are upper limits, because if there is dust present at much lower temperatures than those found from the model fit, it will not emit significantly between 8 and 13 μ and will therefore not contribute to Ω. In fact, the 20-μ flux from IRS 2 (WBN) is larger than would be predicted from the temperature of 270 °K found here, and the 20 μ to 13-μ color temperature is 130 °K. The corrections for silicate absorption at 13 μ and to the broad band 20-μ measurement should be approximately equal (Knacke and Thomson 1973). It is impossible to deduce the true gas

TABLE 4

CLOUD MASSES AND GAS TO DUST RATIOS

Source	Ω arc sec^2	M_d $M_\odot$	$\theta_{H\ II}$* arc sec	$\tau_{em}(9.7)$	M_{gas}* $M_\odot$	M_{gas}/M_d	N_H atoms cm^{-2}
IRS 1	2.6×10^{-1}	1.2×10^{-4}	1.5	1.5×10^{-1}	9×10^{-3}	75	1.3×10^{23}
IRS 2	2.7×10^{-2}	1.2×10^{-5}	9	1.4×10^{-3}	3.6×10^{-1}	3×10^{4}	3×10^{22}
IRS 3	1.6×10^{-2}	7×10^{-6}	2.7	3×10^{-3}	9×10^{-3}	1×10^{3}	5×10^{22}

* from Martin (1973), corrected to d = 3.5 kpc.

to dust ratio without knowing the details of the temperature distribution of the dust, but a normal interstellar ratio of 100 appears consistent with the observations. IRS 3 also has a larger 20-μ flux than would be predicted from the 10-μ observations, and the observations are compatible with a normal gas to dust ratio in this object.

The arguments above would be invalid if a substantial part of the 20 μ flux comes from outside the HII region. Some flux might originate, for example, in the cold material which produces the absorption at 10 μ and the emission at far infrared wavelengths. Any such contribution is probably small, because in IRS 2 the 20 μ and radio maps are in good agreement, and in IRS 1 (see below) the 20 μ flux is no larger than is obtained by extrapolating the 8 to 13 μ flux.

The energy distribution of IRS 1 is different from that of IRS 2 and IRS 3 in that the 20-μ flux is much less relative to the 10-μ flux. The 20-μ, 13-μ, and 5-μ fluxes all fit a 370 ^{o}K blackbody, the same temperature as derived from the 10-μ data alone. The extinction at 5 μ should be about equal to that at 13 μ assuming $A_V/\tau(9.7) = 14$ (Gillett et al. 1975b) and a normal interstellar extinction law (Johnson 1968). It therefore seems that the assumption of a single temperature is reasonable for IRS 1, and the derived gas to dust ratio of 75 is accurate.

The absorption optical depth obtained from the model fit can be used to calculate the column density of material in front of the H II region. The column density can then be used to estimate the total mass outside the H II region. The column density of hydrogen atoms $N_H = f\,\tau(9.7)/K(9.7)\,M_H$ where f is the gas to dust ratio in the cold medium outside the H II region and M_H is the mass of a hydrogen atom. The values of N_H for f = 100 are given in Table 4.

The relation between N_H and the total mass outside the H II region is strongly dependent on how the mass is distributed. The spherically symmetric density distribution requiring the least mass consistent with the measured column density is that in which all the mass is in a thin shell just outside the H II region. This mass is $2\ M_\odot$ for IRS 1. If the material is spread out, the total mass required is larger. For example, if the density $\rho(r) \propto r^{-2}$ from the radius of the H II region r_0 to some maximum radius r_1, the total mass is increased by a factor r_1/r_0. Because the absorption in front of IRS 2 is small, r_1 is less than the distance from IRS 1 to IRS 2. If the projected distance is comparable to the actual distance, the mass is 10 times greater or $20\ M_\odot$.

The effect of the silicate absorption in front of IRS 1 is to remove energy at 10 μ and re-emit it around 100 μ. As discussed above, the 5, 13, and 20-μ fluxes from IRS 1 fit on a 370 ^oK blackbody, so if there were no absorption, most of the luminosity of IRS 1 would emerge around 10 μ. The minimum luminosity of $4 \times 10^4\ L_\odot$ is obtained by assuming that there is no absorption at wavelengths shorter than 8 μ or longer than 3 μ. Correcting the fluxes for absorption, assuming the absorption at 5, 13, and 20 μ is 0.3 of that at 9.7 μ, the luminosity of IRS 1 would be $2.4 \times 10^5\ L_\odot$. If as suggested by the model fits, the underlying spectrum of IRS 1 has a silicate emission feature, the luminosity would be $3 \times 10^5\ L_\odot$. Any of the above luminosities is consistent with a far-infrared measurement by Harper and Thronson (1975) with a field of view which includes all three sources. If a luminosity of $3 \times 10^5\ L_\odot$ is produced by a

zero-age main sequence star, it is of spectral type O6 (Panagia 1973) and mass 35 $M_\odot$ (Cester 1965). Such a star would produce 100 times more ionizing photons than are indicated by the radio observations. Depending on the unknown ratio between the ultraviolet and 9.7 μ optical depths, an optical depth high enough to absorb 99% of the ultraviolet photons may be consistent with the 9.7 μ optical depth of 0.15 inside the ionized region. Another possibility is that the energy of IRS 1 is supplied by a supergiant star; its spectral type is then B0.5, and only 3 times more ionizing photons are produced than would be derived from the radio observations. In either case it appears that a star of 35 $M_\odot$ has formed out of a condensation having total mass between 37 and 55 $M_\odot$.

V. CONCLUSION

The three compact sources in NGC 7538, identified by Martin (1973) as young H II regions, have spectra of two types. IRS1 has a strong silicate absorption, while IRS2 and IRS3 have much weaker silicate absorption. The emission from IRS1 from 5 to 20 μ can be explained with a single temperature for the emitting dust, but in IRS2 and IRS3 a range of temperatures is required. The gas to dust ratio of IRS1 appears to be normal; the observations are probably consistent with normal ratios in IRS2 and IRS3. If older H II regions are dust depleted, the depletion must occur at a later stage of their evolution and is not an initial condition.

It is a pleasure to thank E. E. Becklin and G. Neugebauer for their support and encouragement, including many valuable comments on the manuscript, and C. Sarazin for a discussion of dust depletion mechanisms. S. V. W. Beckwith helped with the observations. This work was supported by National Aeronautics and Space Administration grant NGL 05-002-207 and National Science Foundation grant MPS74-18555.

APPENDIX

In the approximation that the emitting dust particles in a source are all at the same temperature, the observed flux can be written as

$$F_\lambda = \Omega \frac{\epsilon(\lambda)}{\epsilon(9.7)} B_\lambda (T_d) \exp\left[-\tau(9.7)\frac{F_\lambda(\mathrm{Trap})B_{9.7}(T_T)}{F_{9.7}(\mathrm{Trap})B_\lambda(T_T)}\right] \qquad (2)$$

(GFMCS). Here $\epsilon(\lambda)$ is the emissivity and T_d is the temperature of the hot dust, $\tau(9.7)$ is the absorption optical depth at 9.7 μ, $F_\lambda(\mathrm{Trap})$ is the flux from the Trapezium, T_T is the temperature of the dust in the Trapezium, and B_λ is the Planck function. There are four free parameters: Ω, the effective solid angle; T_d; $\tau(9.7)$; and T_T. $F_\lambda(\mathrm{Trap})$ was taken from Forrest, Gillett, and Stein (1975). GFMCS found T_T = 250 K, but T_T = 225 K was used here for reasons discussed below. The applicability of the above model is discussed by GFMCS.

It was found that the only case in which T_T significantly affected the quality of the fit was that for IRS 1 using Trapezium-like emissivity. In this case, T_T = 225 K was at least 2 σ better than either 200 K or 250 K. The emissivity of dust as a function of wavelength is known to be different for different objects (Forrest et al. 1975), and T_T should be regarded as a parameter describing the emissivity of the dust rather than as a physical temperature of the Trapezium. The lower value of T_T found here implies that the emissivity at 7 to 9 μ of the dust in NGC 7538 is larger than that in most of the H II regions studied by GFMCS.

The errors given for T_d and $\tau(9.7)$ are those corresponding to a unit rise in chi-squared per degree of freedom. This corresponds to the standard deviation rather than the standard deviation of the mean and should be a better estimate of the error when, as here, the error is not primarily statistical. This method of estimating the error in T_d and $\tau(9.7)$ should be accurate because T_d and $\tau(9.7)$ are not correlated. T_d does depend on T_T, and Ω depends strongly on T_d. Increasing T_T by 25 K increases Ω by about a factor of 3.

REFERENCES

Aitken, D. K., Jones, B., and Penman, J. 1974, in H II Regions and the Galactic Centre: Proceedings of the Eighth ESLAB Symposium, Frascati, Italy, ed. by A.F.M. Moorwood, p. 43.

Cester, B. 1965, Z. Ap., 62, 191.

Downes, D., and Wilson, T. L. 1974, Ap. J. (Letters), 191, L77.

Forrest, W. J., Gillett, F. A., and Stein, W. A. 1975, Ap. J., 195, 423.

Gillett, F. C., and Forrest, W. J. 1973, Ap. J., 179, 483.

Gillett, F. C., Forrest, W. J., Merrill, K. M., Capps, R. W., and Soifer, B. T. 1975a, in press.

Gillett, F. C., Jones, T. W., Merrill, K. M., and Stein, W. A. 1975b, in press.

Goldman, A. 1970, Appl. Optics, 9, 2,600

Harper, D. A. and Thronson, H. A., 1975, private communication.

Israel, F. R., Habing, H. J., and de Jong, T. 1973, Astron.and Astrophys., 27, 143.

Johnson, H. L. 1968, in Nebulae and Interstellar Matter, eds. B. M. Middlehurst and L. H. Aller (Chicago: University of Chicago Press), p. 193.

Knacke, R. F., and Thomson, R. K. 1973, P.A.S.P., 85, 341.

Martin, A. H. M. 1973, M.N.R.A.S., 163, 141.

McClatchey, R. A., Fenn, R. W., Selby, J. E. A., Volz, F. E., and Garing, J. S. 1972, Optical Properties of the Atmosphere (3rd edition; Air Force Cambridge Research Laboratories, Report AFCRL-72-0497).

Morris, M., Palmer, P., Turner, B. E., and Zuckerman, B. 1974, Ap. J., 191, 349.

Panagia, N. 1973, Ap. J., 78, 929.

Persson, S. E., and Frogel, J. A. 1974, Ap. J., 188, 523.

Petrosian, V. 1970, Ap. J., 159, 833.

Thaddeus, P., Kutner, M. L., Penzias, A. A., Wilson, R. W., and Jefferts, K. B. 1972, Ap. J. (Letters), 176, L73.

Turner, B. E., Zuckerman, B., Palmer, P., and Morris, M. 1973, Ap. J., 186, 123.

Wilson, W. J., Schwartz, P. R., Epstein, E. E., Johnson, W. A., Etcheverry, R. D., Mori, T. T., Berry, G. G., and Dyson, H. B. 1974, Ap. J., 191, 357.

Wynn-Williams, C. G., Becklin, E. E., and Neugebauer, G. 1974, Ap. J., 187, 473.

Wynn-Williams, C. G., Werner, M. W., and Wilson, W. J. 1974, Ap. J., 187, 41.

CHAPTER 2

THE GALACTIC CENTER

I. INTRODUCTION

The region of the Galactic center is very bright in the infrared, both at relatively short wavelengths of 1 to 20 μ (Becklin and Neugebauer 1968, Low et al. 1969) and at longer wavelengths near 100 μ (Hoffmann, Frederick, and Emery 1971). At the shorter wavelengths, maps have revealed a concentration of discrete sources in a region approximately 1' in diameter (Rieke and Low 1973). Maps with better spatial resolution have shown more sources, and many of the sources have finite sizes of approximately 2" or 0.1 pc (Becklin and Neugebauer 1975--hereafter BN).

The position of the infrared sources is the same as that of the thermal radio source Sgr A-West, but even the highest resolution radio map (Ekers et al. 1975) is not sufficient to allow a detailed comparison with the infrared maps. The radio emission indicates the presence of an H II region in the Galactic center; an emission line of Ne II at 12.8 μ (Aitken, Jones, and Penman 1974) presumably arises from the same region. The far infrared radiation is probably due to the presence of dust in or near the H II region.

The present paper presents new observations of three kinds: a 10-μ map with 2".3 resolution over a broader region than that of BN, broad and intermediate bandwidth photometry of individual sources, and 8 to 13-μ spectrophotometry of individual sources. The new data are interpreted in terms of the properties of individual sources, the relationship of the compact sources to the large scale structure, and the amount and wavelength dependence of the interstellar extinction.

II. OBSERVATIONS

A revised and extended version of the 10-μ map of BN is presented in Figure 1. New data, consisting of scans to the east of the center of IRS1, were obtained on 1975 July 1. The observation and reduction procedure was the same as that of BN. In addition, in the process of making the photometric measurements described below, the relative positions of the discrete 10-μ sources were measured. The new positions have been incorporated into Figure 1; the most significant change is that IRS3 is closer to IRS7 than was indicated by BN. The absolute coordinates of the map were also checked using the optical field star indicated by an "X". The check revealed a difference of about 2" in the sense that the declinations presented here are south of the values listed by BN. The difference is probably due to the difficulty of accounting for the effects of differential refraction.

The 1.2 to 12.5-μ broadband observations were made at the 5-m Hale telescope on four nights in 1975 June and July. The 1.2 to 5-μ observations were made with an InSb detector, a 3".8 aperture, and a conventional chopper producing a 7".5 beam separation in declination. The 8.7 to 12.5-μ observations used a bolometer detector, a 2".3 aperture, and a wobbling secondary chopper producing a 10" beam separation in declination. The seeing was generally 2" for the short wavelength and 3" for the long wavelength observations. The source positions were found by peaking up on individual sources; the spatial resolution was approximately the same as BN used to make the 2.2 and

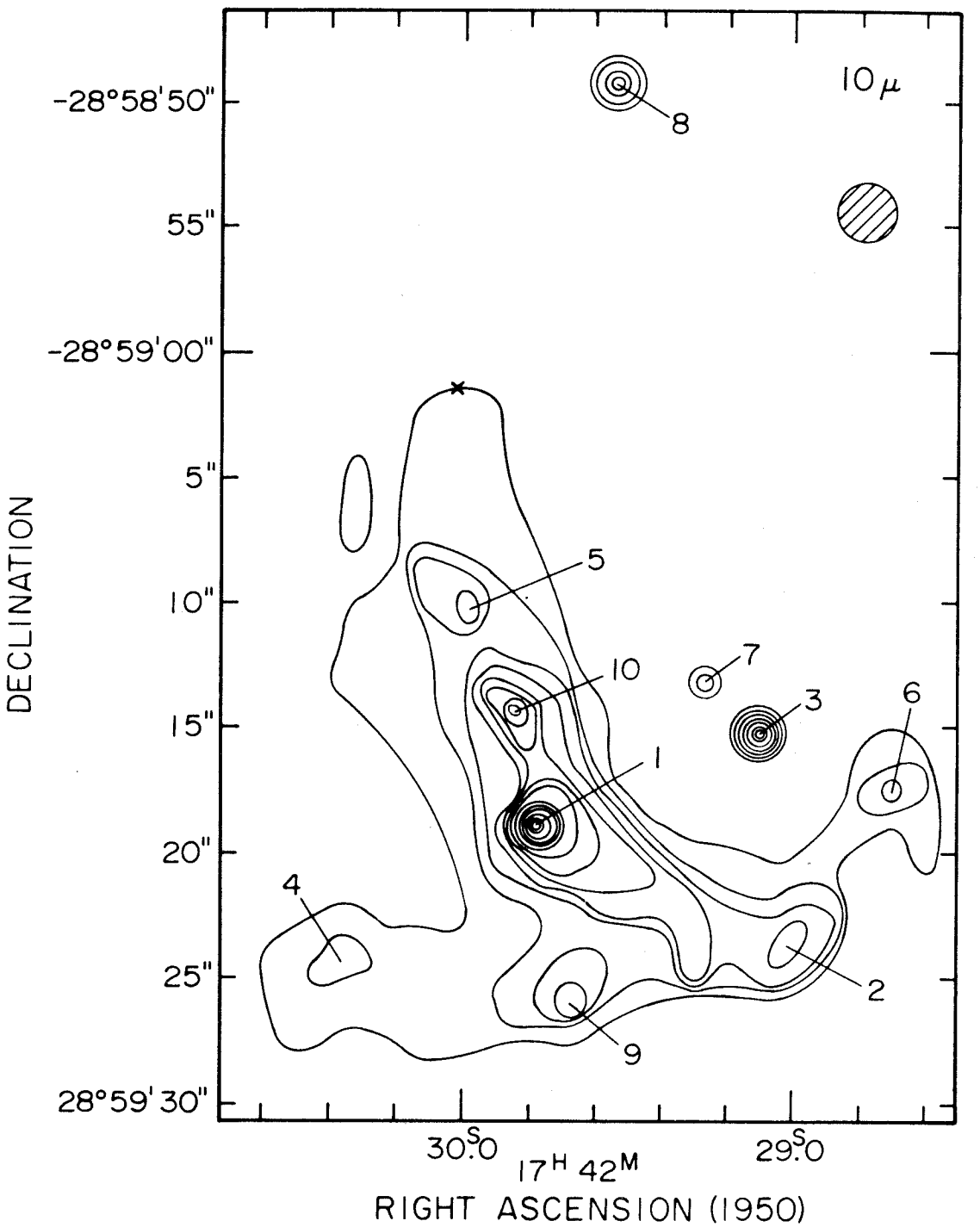

Figure 1

Map of the Galactic center region at 10 μ made with a 2".3 circular aperture. The aperture size is shown by the circle in the upper right hand corner. The "X" denotes a visible field star. The IRS numbers are shown. The contour interval is 4 x 10^{-16} W m^{-2} Hz^{-1} $ster^{-1}$.

10-μ maps of the Galactic center, so the sources were easily located. The location of the reference aperture was chosen to minimize contamination. In one case, that of IRS16, it was necessary to measure the flux in the reference position and correct the data appropriately. The results of the photometry, in magnitudes, are given in Table 1, which also gives 20-μ magnitudes determined from an unpublished map by Becklin and Neugebauer. The major sources of error are errors in centering the aperture on the source and errors due to unknown flux in the reference beam. Centering errors were less than 0.2 magnitudes, as indicated by remeasurement of some of the sources on different nights. Errors due to flux in the reference beam depend on how isolated the source being measured is; such errors are difficult to estimate. As an extreme upper limit, the flux in the reference beam when measuring IRS16 amounted to 0.6 magnitudes.

Spectral observations were made in 1974 August and September, but most of the data were obtained on seven nights in 1975 May and June. The observations were made at the 2.5-m Hooker telescope and used a 5" aperture and a 17".5 beam separation in declination. The source positions were found by peaking up with a broadband filter; the positions measured are shown in Figure 2 superposed on the 10-μ map. The seeing was very good on most of the nights, being typically 2" when observing the Galactic center. The observation and reduction techniques were the same as described previously (Chapter 1) except that the star used to determine absolute fluxes was α Sco; its 12.5-μ flux was assumed to be 1.80×10^{-23} Wm^{-2} Hz^{-1}. The results of the spectral observations are given in Figure 3.

TABLE 1

OBSERVATIONS AND ADOPTED EXTINCTION CORRECTIONS

Source	1.2μ	1.65μ	2.2μ	3.4μ	4.8μ	8.7μ	9.5μ	11.2μ	12.5μ	20μ*
1		11.1	8.4	5.4	3.8	0.4	0.8	-0.7	-1.5	-2.6
2						1.7	2.2	0.5	-0.8	-0.8
3				5.1	2.8	0.9	2.6	0.7	-0.9	0.0
4						3.4	4.1	1.7	0.3	
5						2.0	2.7	1.0	0.1	-1.5
6						1.9	2.7	1.0	-0.5	0.0
7	13.8	9.2	6.6	4.6	4.3	3.0	4.2	2.4	0.7	> 0.0
8		15.3	10.1	6.1	4.2	1.4	2.4	1.0	-0.2	-0.8
9		11.1	8.7	6.4	4.6	1.6	2.3	0.5	-0.8	-1.2
10						1.0	1.6	0.2	-0.8	-1.9
11		10.9	8.8	7.2	6.5†					
12‡		10.3	8.0	5.7	4.0					
16		10.4	8.3	6.4	4.6†					
19‡		10.6	8.1	6.5	6.3†					
Adopted Extinction Correction	8.4	4.7	2.6	1.1	0.8	2.2	3.7	2.3	1.3	1.1

* From unpublished map by Becklin and Neugebauer.

† Statistical error 0.4 (IRS11), 0.1 (IRS16), and 0.3 (IRS19).

‡ Measured with 5" aperture.

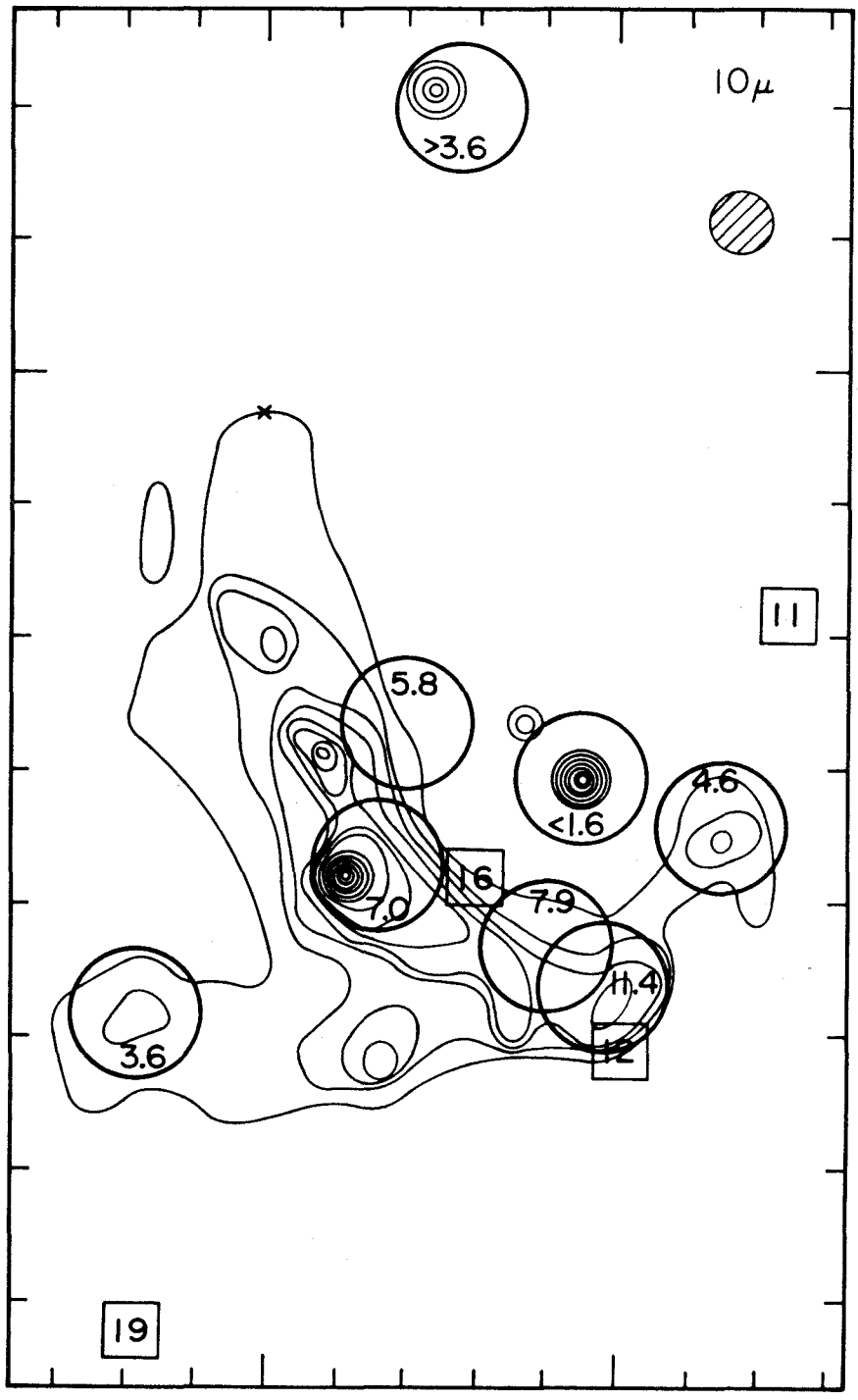

Figure 2

The positions and size of the 5" spectrometer aperture superposed on the 10-μ map. The numbers inside the circles denoting the aperture locations give the measured Ne II flux in units of 10^{-18} W m^{-2}. The squares mark the central positions of 2-μ sources that do not appear on the 10-μ map; the numbers inside the squares are the IRS numbers.

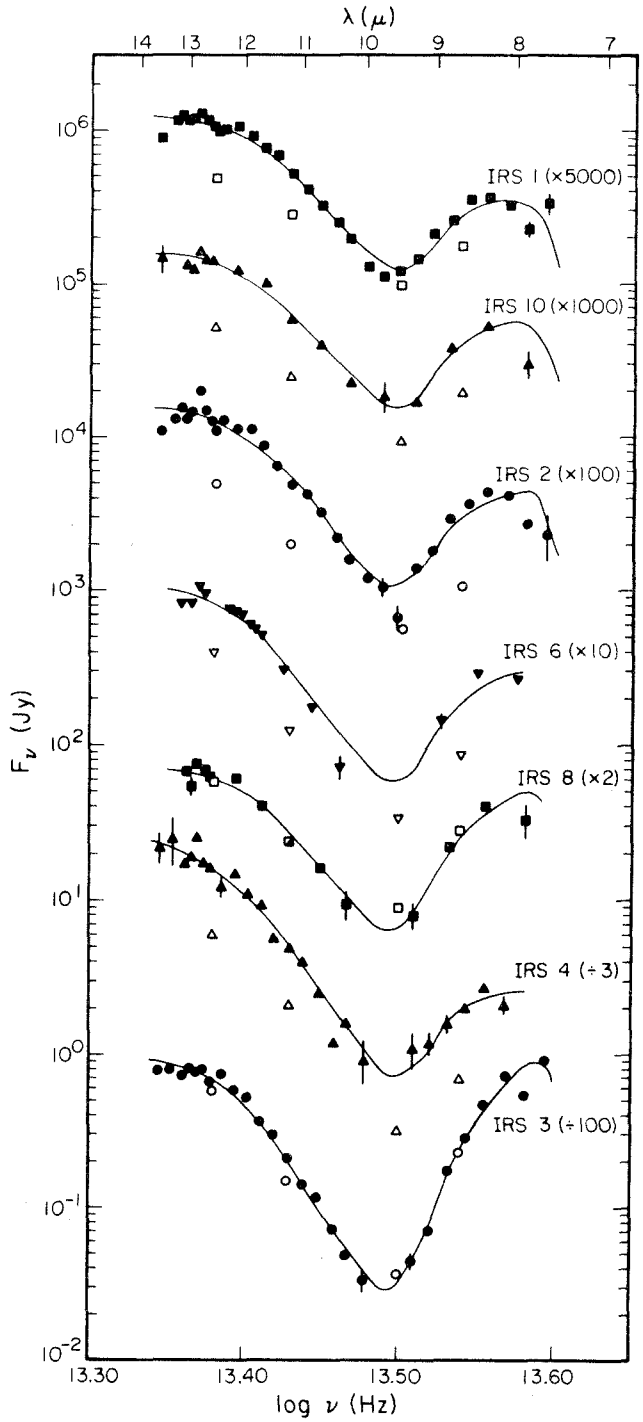

Figure 3

Observed fluxes from 7.5 to 13.5 μ. Filled symbols represent the spectrometer observations and open symbols the broadband observations. Error bars are given for points whose statistical error exceeds 10%. The lines represent fits to the spectrometer observations.

III. DISCUSSION

a) Extinction at Short Wavelengths

In order to discuss the nature of the sources in the Galactic center, it is necessary to correct the observations for interstellar extinction. The data presented here give information on both the uniformity and the magnitude of the extinction. Becklin and Neugebauer (1968) have shown that the [1.6μ] - [2.2μ] color measured through 15" to 110" apertures centered on the 2.2-μ peak is uniform, although the total flux increases by a factor of 8. They attributed the flux to a background of unresolved stars. In addition, the present observations show that four compact sources in the central region--IRS11, 12, 16, and 19--have the same [1.6μ] - [2.2μ] color as the 110" region to within 15%. These sources have no 10-μ counterparts; the lack of 10-μ radiation from these sources and the presence of 2.3-μ CO absorption in two of them (Neugebauer et al. 1976) indicate that the sources are probably stars. These sources are distributed over a 40" area, as shown in Figure 2, and their total 2.2-μ flux is only 3% of that in the 110" aperture. The uniformity of the observed colors of these four sources and the equality of the colors to that of the 110" region show that there is a uniform component of the extinction towards the Galactic center. The uniform extinction is the minimum to any source in the Galactic center.

If the 2.2-μ compact sources are distributed symmetrically around the Galactic center, the uniformity of their colors implies that there

is little reddening in the immediate vicinity of the center. The fact that the unresolved stars within 55" have the same color can be taken to show that there is little reddening within the radius of the extended source. Quantitatively, the reddening varies by less than 0.4 magnitudes even if there is some dispersion in the intrinsic color of the sources. The color excess, given below, is 2.1 magnitudes, so at most 20% of the extinction could be within the central 55" or 2.5 pc radius of the Galactic center.

If the extinction is interstellar, it is extremely unlikely that there are any holes having substantially less extinction than the average. It should be pointed out that some localized areas less than 2" in diameter of higher than average extinction cannot be ruled out, especially if such an area is associated with a 2-μ source. The uniformity of the extended emission shown in the 2.2-μ map of BN indicates that such areas are not common.

The observation with the 110" aperture (Becklin and Neugebauer 1968) gives a [1.6μ] - [2.2μ] color of 2.25 magnitudes. If the intrinsic color is the same as that of the central regions of M31 (Sandage, Becklin, and Neugebauer 1969), the color excess is 2.10. This excess was converted into an absorption at 1.25, 1.65, 2.2, 3.5 and 4.8 μ using an average extinction curve similar to van de Hulst's curve 15 (Table 1). Figure 4 shows the fluxes of the four compact sources from 1.6 to 4.8 μ after correction for extinction. The bluest sources, IRS11 and 19, are approximately Rayleigh-Jeans from 1.6 to 4.8 μ; the reddening curve used is therefore consistent with the

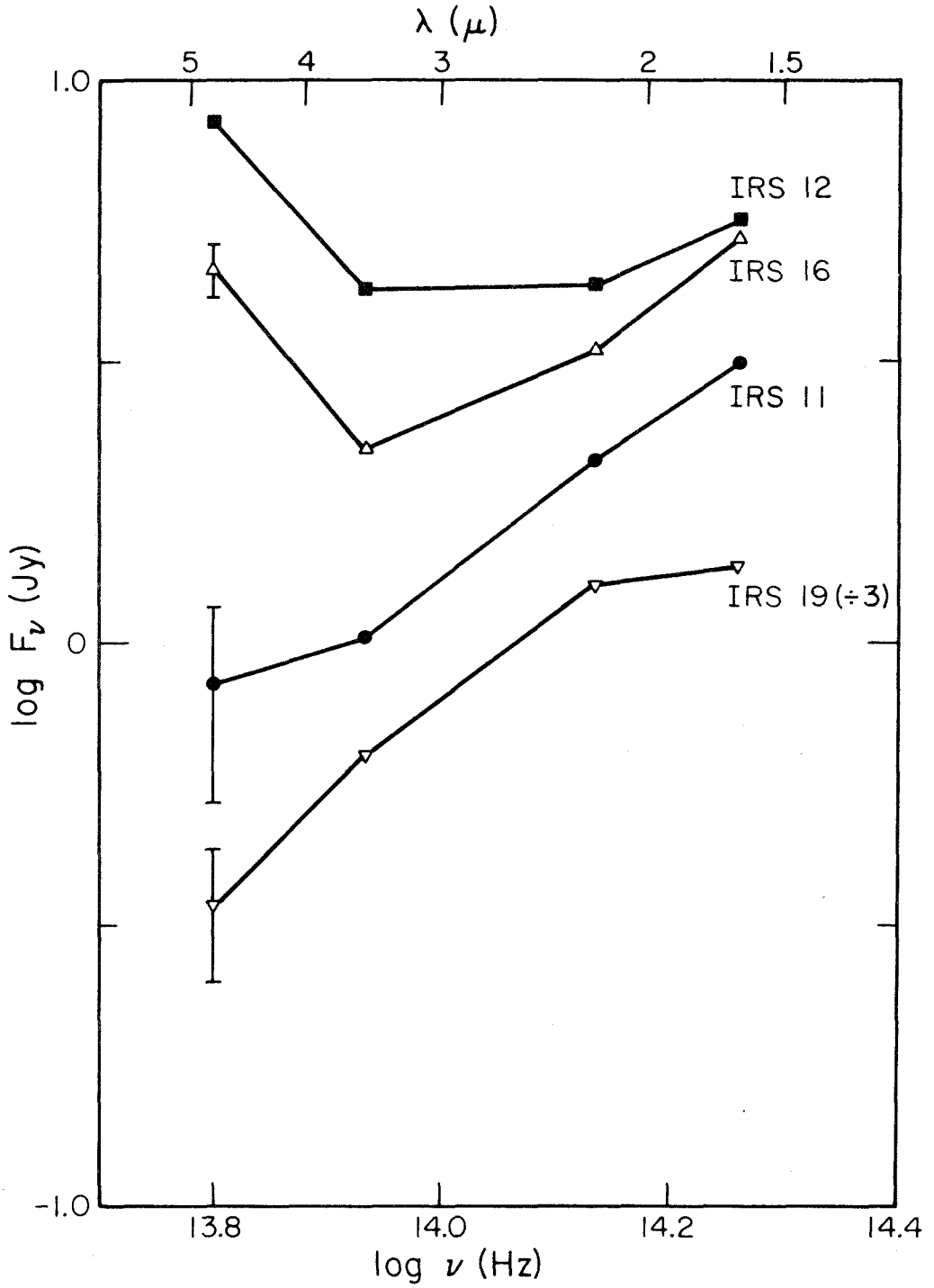

Figure 4

Corrected energy distributions for four sources with no 10-μ counterparts. Error bars are given for points whose statistical error exceeds 10%.

observations at these wavelengths. The energy distributions of IRS12 and 16 are discussed in sub-section d; here it suffices to say that other sources in the aperture may contribute most of the 3.5 and 4.8-μ flux. As discussed in sub-section c, if the same reddening curve is applied to IRS7, this source has an energy distribution like that of an M supergiant from 1.2 to 4.8 μ; thus the consistency of the extinction curve extends to 1.2 μ. The visual extinction A_V corresponding to a color excess of 2.10 is 28 magnitudes.

b) Silicate Extinction

In order to correct the 8 to 20-μ observations, it is necessary to account for silicate absorption, which dominates the extinction. Hackwell, Gehrz, and Woolf (1970), using a 10" aperture, found an absorption feature near 10 μ in the Galactic center, and the present observations show a feature at least as strong in all ten of the sources observed near 10 μ. It is impossible to correct for the absorption directly, because the underlying energy distribution is not known for any source; this contrasts sharply with the situation at shorter wavelengths, where the bluest sources can be assumed to follow a nearly Rayleigh-Jeans energy distribution. The shape of the silicate absorption seems to be nearly the same in a large variety of objects (Willner 1976 and references therein); a typical shape is given in Table 2.

The observations were fit by applying the extinction curve of Table 2 to two extreme underlying spectra. Table 3 gives the derived amount of silicate absorption $\tau(9.7)$ towards each of the ten sources observed

TABLE 2

RELATIVE SILICATE OPTICAL DEPTH*

λ μ	$\tau(\lambda)$	λ μ	$\tau(\lambda)$
7.75	0.15	11.00	0.68
8.00	0.29	11.25	0.61
8.25	0.43	11.50	0.54
8.50	0.53	11.75	0.48
8.75	0.62	12.00	0.42
9.00	0.79	12.25	0.38
9.25	0.92	12.50	0.35
9.50	0.99	12.75	0.31
9.75	1.00	13.00	0.28
10.00	0.94	13.25	0.26
10.25	0.89	13.50	0.23
10.50	0.82	13.75	0.22
10.75	0.77		

* Normalized to $\tau(9.7) = 1.0$.

TABLE 3

ABSORPTION AT 9.7 μ*

Source	If Silicate Emission		If Blackbody Emission†	
	Broad Bandwidth Observations	Narrow Bandwidth Observations	Broad Bandwidth Observations	Narrow Bandwidth Observations
1	3.7	4.4	2.1	2.3
2	4.1	4.9	2.6	2.8
3	6.5	6.9	5.0	4.6
4	5.0	5.3	3.4	3.1
5	4.1	---	2.7	---
6	4.9	5.3	3.4	3.0
7	5.6	---	4.1	---
8	4.8	5.3	3.2	3.1
9	4.5	---	2.9	---
10	4.1	4.6	2.6	2.5

* In magnitudes.

† Or emissivity proportional to λ^{-1}.

with broadband photometry. Seven of these sources were also observed with the spectrometer; the lines in Figure 3 represent the fits to the spectrometer data. Columns 2 and 3 of Table 3 are based on the assumption that the underlying spectrum shows a strong silicate emission feature like that of the Orion Trapezium, while columns 4 and 5 are based on an underlying blackbody spectrum. In each case, the value for the source temperature best representing the 8 to 13-μ observations was assumed; these values ranged from 200 to 600 K. The source temperatures assumed made little difference to the optical depths determined from the narrow bandwidth observations, but the optical depths determined from the broader bandwidth observations are uncertain by 0.3 because of the uncertainty in the temperatures. The errors given by the fits range from 0.2 to 0.4, but the real uncertainty in the optical depths is due to the fact that the underlying spectrum is unknown. The assumption of an underlying silicate emission feature should give an upper limit on the optical depth, while the assumption of a smooth underlying spectrum gives a lower limit.

The extinction curve given in Table 2 has about 30% as much absorption at 8 and 13 μ as at 9.7 μ. This value is very uncertain; it could range from below 10% to about 50%. The absolute 10-μ fluxes are therefore uncertain by about a factor of 3, as are the short wavelength to 10-μ colors.

The difference between the optical depths measured with broad and narrow bandwidths arises from two causes. Firstly, the 9.5-μ broadband measurement refers to the average flux over approximately

a 1-μ bandwidth; because the flux is a minimum near 9.5 μ, as shown in Figure 3, the average is higher than the actual 9.5-μ flux. The spectrometer observations are not significantly affected because of their smaller bandwidth. Secondly, there is an extremely red background around some of the sources. Because of the larger aperture used for the spectrometer observations, the measured flux at wavelengths longer than 11 μ is too large. The background can be seen in the observations of IRS1 presented in Figure 3; the effect of the background is to lower the temperatures and raise the optical depths derived from the spectrometer observations. If the reasons for the differences between the narrow and broadband optical depths are considered, it seems that the narrow band optical depths best represent the true extinction to the sources, except in the sources which are significantly contaminated by background flux in the larger aperture. In these sources, IRS1 and 10, some average of the narrow and broadband optical depths should be used.

The values of $\tau(9.7)$ that were derived under the assumption of blackbody emissivity represent lower limits to the total silicate absorption to each source listed in Table 3. If it can be shown that any source has no intrinsic silicate absorption, the value of $\tau(9.7)$ to that source will be a lower limit to the interstellar absorption. As discussed below, IRS7 appears to be a star surrounded by a dust shell, which emits at 10 μ. In order for IRS7 to have significant intrinsic absorption, the 9.7-μ optical depth of the dust shell would have to be much greater than unity, because for small optical depths

the silicate feature appears in emission; the emission feature only disappears when the optical depth is greater than approximately 1. From the short wavelength observations, the 2.2-μ optical depth of the dust shell appears to be only 0.3 magnitudes (sub-section c). Day, Steyer, and Huffman (1974) present laboratory measurements of the visual and 10-μ extinction cross-sections of amorphous quartz. If the ratio of 5890 Å to 2.2-μ extinction of the quartz is the same as that of visual to 2.2-μ given by the extinction curve adopted above, a 2.2-μ absorption of 0.3 could imply a 9.7-μ absorption of 1.5 magnitudes. Such a large value was, however, found only for the single most extreme sample; more typical values imply a factor of 6 less 9.7-μ absorption. Mie theory calculations by Day et al. showed that the ratio of 9.7-μ to visual, and presumably to 2.2-μ, extinction depends on particle size and composition. The largest calculated 9.7-μ to visual extinction would imply about 2 magnitudes of silicate absorption to IRS7. Either larger or smaller particles, or a different composition, would reduce the amount of absorption. Furthermore, a ratio of 9.7 to 2.2-μ extinction as large as the largest calculated by Day et al. has not been observed in any astronomical object. Finally, even a total optical depth of 2 would produce only about 1 magnitude of apparent silicate absorption, because of filling in by silicate emission. Thus, it appears that the interstellar extinction at 9.7 μ is greater than or equal to 3.6 magnitudes; the difference between this value and the value of 4.1 given for IRS7 in Table 3 is due to the presence of 12% more extinction to IRS7 than the adopted interstellar amount.

The value of $\tau(9.7) \geq 3.6$ is consistent with the values of $\tau(9.7)$ for IRS1, 2, 5, and 10 only if those sources have an underlying spectrum with a silicate emission feature. The minimum optical depth to any of those sources for the broader bandwidth observations is $\tau(9.7) = 3.7$ magnitudes, and this value has been adopted as the minimum 9.7-μ absorption to sources in the Galactic center. The absorption corrections at 8.7, 9.5, 11.2, and 12.5 μ are given in Table 1.

Attention should be drawn to the anomalous [11.2μ] - [12.5μ] color for IRS7, as shown in Figure 5. Possibly the form of the extinction curve assumed is incorrect; this seems unlikely because of the good fits to the observations of other sources. Another possibility is that there is more extinction to IRS7 than was assumed, in which case IRS7 would have a silicate emission feature. Uncertainties of the size of the anomaly in IRS7 are inherent in the extinction correction.

The extinction correction at 20 μ is even less certain than the total amount of 10-μ extinction. The best estimate that can be made at present is from laboratory measurements of lunar rocks and meteorites (Knacke and Thomson 1973, Penman 1976). The optical depth averaged over the band pass of the 20-μ filter appears to be at least 0.3 of $\tau(9.7)$, but this correction may be too small.

c) IRS7

IRS7 is one of the most interesting sources in the Galactic center region. At 2.2 μ, it is four times brighter than any other source within 1.5 pc of the Galactic center (BN); after correction for interstellar reddening (see Figure 5), it has a blue spectrum from 1.2 to 4.8 μ. The presence of CO in absorption at 2.3 μ suggests that the source is a star, but the source is considerably brighter at 10 μ than would be expected from extrapolating the short wavelength observations. Figure 5 shows the 1 to 20-μ energy distribution of IRS7 corrected for interstellar extinction; also shown for comparison are the energy distributions of HD143183 (Humphreys and Ney 1974) and

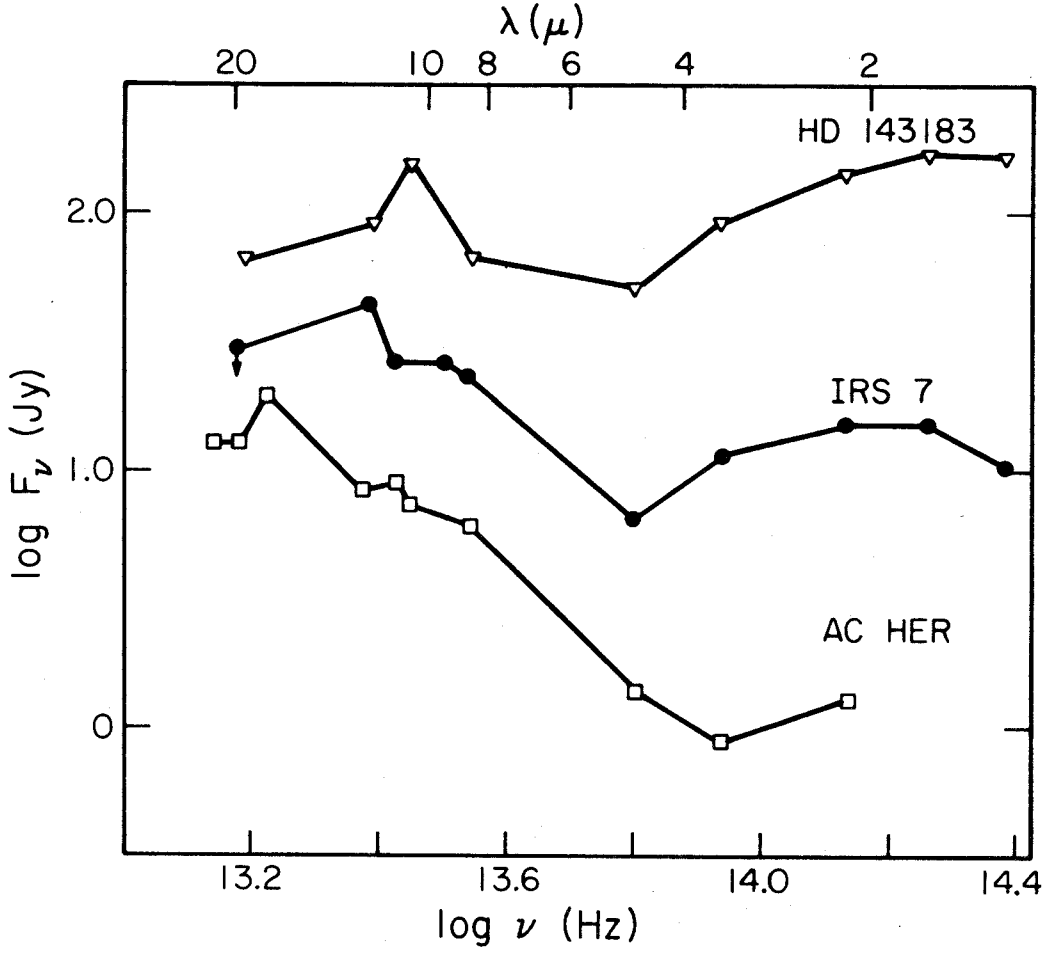

Figure 5

Energy distribution of IRS7 corrected for extinction. Also shown are the energy distributions of two stars; measurements of HD143183 are from Humphreys and Ney (1974), and those of AC Her are from Gehrz (1972). The fluxes of HD143183 were corrected for reddening and adjusted to a distance of 10 kpc, thec multiplied by 3 for convenience in plotting. The fluxes of AC Her are in arbitrary units.

AC Her (Gehrz 1972). HD143183 is an M3 Ia supergiant; if this star were observed at the distance of the Galactic center it would be three times brighter at 2.2 μ than IRS7. AC Her is an RV Tauri star with an unusual energy distribution; the reddening and distance are unknown, so its flux is plotted in arbitrary units.

All three sources plotted in Figure 5 have similar energy distributions. The spectra rise from 3.5 to 2.2 μ, wavelengths where the flux is emitted by the stellar photospheres. The spectra also rise toward wavelengths longer than 5 μ; this emission is probably due to optically thin circumstellar dust shells. The excess in IRS7 is not an artifact of the extinction correction; even with no correction near 10 μ there is still excess emission. An additional reddening correction amounting to 12% of the total would make the 1.2 to 5-μ energy distribution of IRS7 almost identical to that of HD143183. IRS7 would then be intrinsically fainter than HD143183 by a factor of 2.5; the luminosity of IRS7 is about 10^5 $L_\odot$. There might be an error in the distance to HD143183 (Humphreys and Ney 1974), but stars as intrinsically bright at 2 μ and as luminous as IRS7 certainly exist. Although the total extinction at 10 μ is very uncertain, it appears that IRS7 has a larger excess than HD143183, but less than AC Her. The apparent absence of a silicate emission feature in IRS7 might be due to an underestimate of the silicate extinction, or the composition of the dust shell could be carbon-rich, as is the case for AC Her (Gehrz 1972). In summary, it appears that IRS7 has the properties of a late-type supergiant situated at the Galactic center.

d) Stellar Sources - IRS11, 12, 16, and 19

In addition to IRS7, four of the sources observed are brighter, after correction for absorption, at 1.6 μ than at 2.2 or 3.5 μ. The corrected energy distributions of these sources, IRS11, 12, 16, and 19, are shown in Figure 4. CO absorption has been observed in IRS11 and 12 (Neugebauer et al. 1976), but not in IRS16; IRS19 was not observed. As mentioned in sub-section a, the fact that the corrected colors are close to 0 and the presence of CO absorption in two of them suggest that these four sources are stars or star clusters.

The spectra of these sources differ at wavelengths longer than 3 μ with those of IRS11 and 19 continuing to decrease, while those of IRS12 and 16 increase. Some or all of the increase in IRS12 and 16 may be due to contamination from other sources; as shown in Figure 2, IRS12 is near IRS2, and IRS16 is near the ridge between IRS1 and 2. The long wavelength turn-up, if not due to contamination, could be due to dust mixed in with the stars or to non-thermal processes. In this regard, there is a non-thermal source near the position of IRS16 (Balick and Brown 1974, Lo et al. 1975).

e) Ridge Sources - IRS1, 2, 5, 6, 9, and 10

In order to determine the relationship between the compact infrared sources and the thermal radio source Sgr A-West, observations of the Ne II line at 12.8 μ must be used as a substitute for radio continuum observations, because the presently available radio observations do not have sufficient spatial resolution. The Ne II emission is

proportional to the free-free radio emission, provided the neon abundance and fractional ionization are constant.

Table 4 gives the Ne II flux as observed in 5" apertures centered on seven of the 10-μ sources and on one position on the ridge. Figure 2 shows, superposed on the 10-μ map, the positions of the apertures and the Ne II flux measured in each one. The continuum fluxes measured agree with those of Rieke and Low (1973), if allowance is made for the difference in the wavelength of observation. The continuum fluxes agree less well with the present 10-μ map, because the small aperture and small chopper spacing with which the map was made tend to cancel extended features.

Several points about the distribution of Ne flux can be noted. First, the Ne flux peaks on the ridge of emission that extends from IRS5 to 1 and to 2. This is in general agreement with the radio observations (Ekers et al. 1975), which have lower angular resolution. Second, there is little or no Ne emission north of the ridge. Third, the intensity of the Ne emission along the ridge is not correlated with the presence of individual 10-μ sources, in particular IRS1. This can be seen from Table 4, which shows that the Ne equivalent width in IRS1 is only half that of the other sources along the ridge. Furthermore, the Ne equivalent width measured with a 25" aperture is 0.035 μ (Aitken et al. 1976) compared to less than 0.030 μ for most of the sources along the ridge. That the compact sources do not contribute much to the Ne flux is in agreement with the radio observations (Ekers et al. 1975), which showed that at most 10% of the radio flux comes from

TABLE 4

Ne II OBSERVATIONS

Source	Observed Ne II Flux (10^{-18} W cm^{-2})	Corrected Ne II Flux (10^{-18} W cm^{-2})	Equivalent Width (10^{-3} μ)
1	7.0 ± 1.3	23	16
2	11.4 ± 0.9	44	42
3	< 1.6	< 10.9	< 11
4	3.6 ± 0.7	15.7	36
6	4.6 ± 1.2	19.4	28
8	< 3.6	15.7	< 63
10	5.8 ± 1.3	21	24
8" S. of 7	7.9 ± 1.6	27	28
Total*	75	250	35

* 25" aperture (Aitken et al. 1976).

sources less than 10" in diameter. Fourth, the total flux measured is only about 40×10^{18} W m^{-2}, even if allowance is made for sources that were not measured such as IRS5. This is significantly less than the 75×10^{-18} W cm^{-2} measured with a 25" aperture (Aitken et al. 1976), indicating that a large part of the Ne emission arises from an extended source. As further evidence for an extended source, Wollman et al. (1976) have detected significant Ne II emission from regions 20" or more north and south of the 10-μ concentration, and the radio observations (Ekers et al. 1975) directly indicate the presence of an extended region of ionized hydrogen.

The distribution of the Ne line flux allows several conclusions to be drawn. First, because the Ne surface brightness is roughly constant along the ridge, the density of ionized gas must also be approximately constant, unless abundance or ionization effects exactly cancel the effects of different densities. The gas density may decrease to the north and south of the ridge. The detection of Ne II apparently not associated with any discrete 10-μ source implies that the H II regions are density rather than ionization bounded; it is therefore likely that the whole region near the Galactic center is ionized.

Second, the 10-μ sources must represent individual sources of energy, if the gas to dust ratio is constant. Because the density is constant, the continuum infrared flux can increase only where the dust particles are hotter, i.e., where they are near an energy source. The heated regions have a typical size of 0.1 pc, comparable to that of compact H II regions. The energy distributions of the ridge sources are also

similar to those of compact H II regions, as shown in Figures 6 and 7. The sources differ from compact H II regions in having less 20-μ flux relative to 10 μ, as shown in Figure 6, little or no Ne II emission, as shown in Figure 2 and Table 4, and little or no intrinsic silicate absorption, as shown in Figure 7. While examples of compact H II regions having one or even two of the above properties exist, no example having all three is known; the 10-μ sources in the Galactic center are therefore not normal compact H II regions.

Third, there are at least two possible sources of the ionizing photons that must be present in the Galactic center. One possibility is that the 10-μ sources are also the sources of ionization, but the nearly constant Ne surface brightness suggests that this is not the case. Small variations in the Ne surface brightness are, however, present, and the 10-μ sources cannot be ruled out as supplying the ionizing radiation. Another possibility is that the ionization is due to a single source. The ridge is shaped like an arc with a non-thermal radio source (Balick and Brown 1974) near the center. The lack of Ne II flux near IRS3 could be caused by the neon being doubly ionized in that region.

The mass of emitting dust in the sources can be crudely estimated from the fitting procedure used to get the silicate absorption. The fit to the 8 to 13-μ observations gives the temperatures, which range from 200 to 600 K. Dust masses of order 10^{-4} $M_{\odot}$ were derived; the 9.7-μ absorption coefficient of the dust was taken to be 3×10^{3} cm^{2} g^{-1} (Gillett and Forrest 1973). The ratio of the mass of gas to the mass

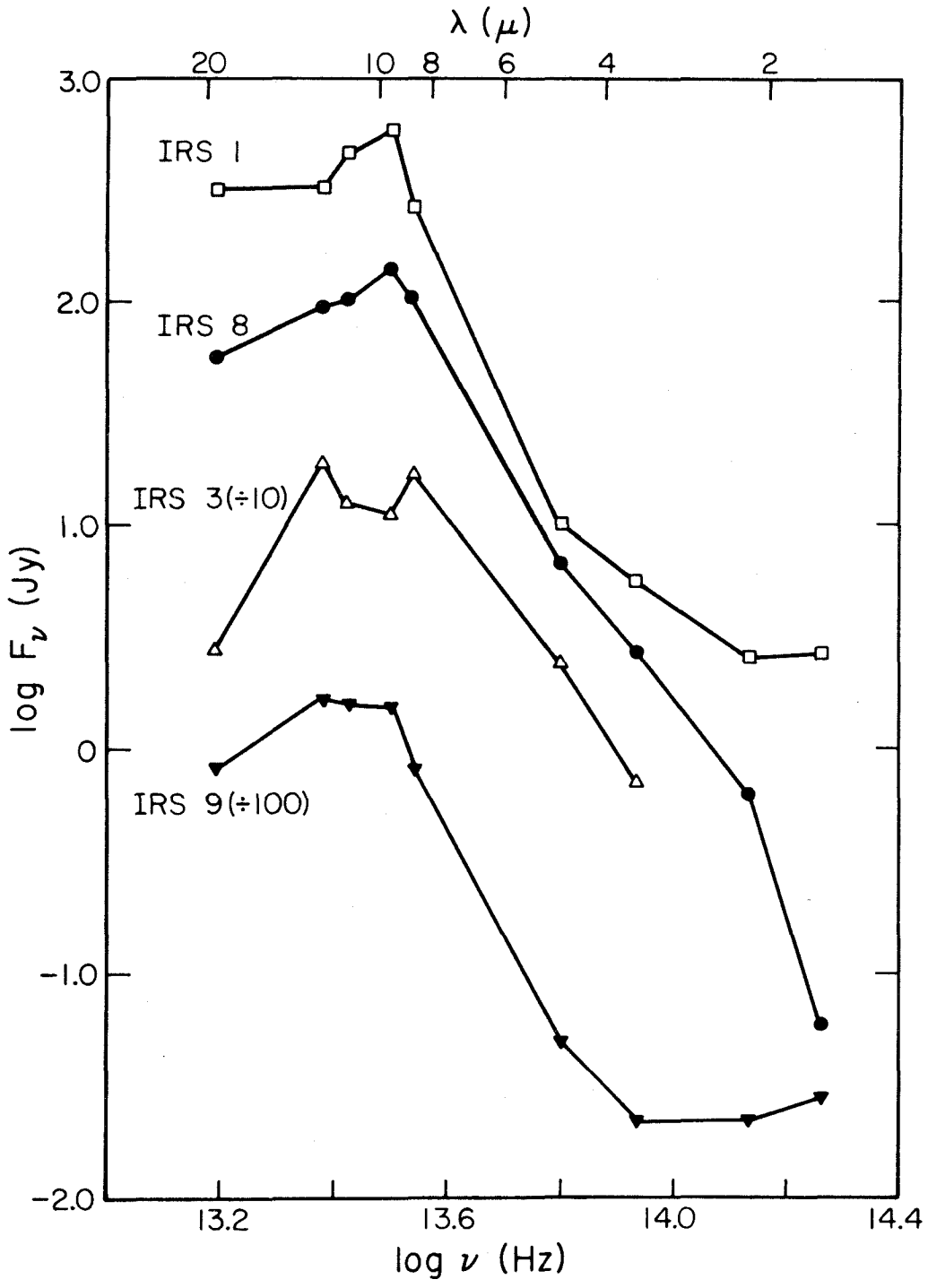

Figure 6

Energy distributions corrected for extinction of four sources.

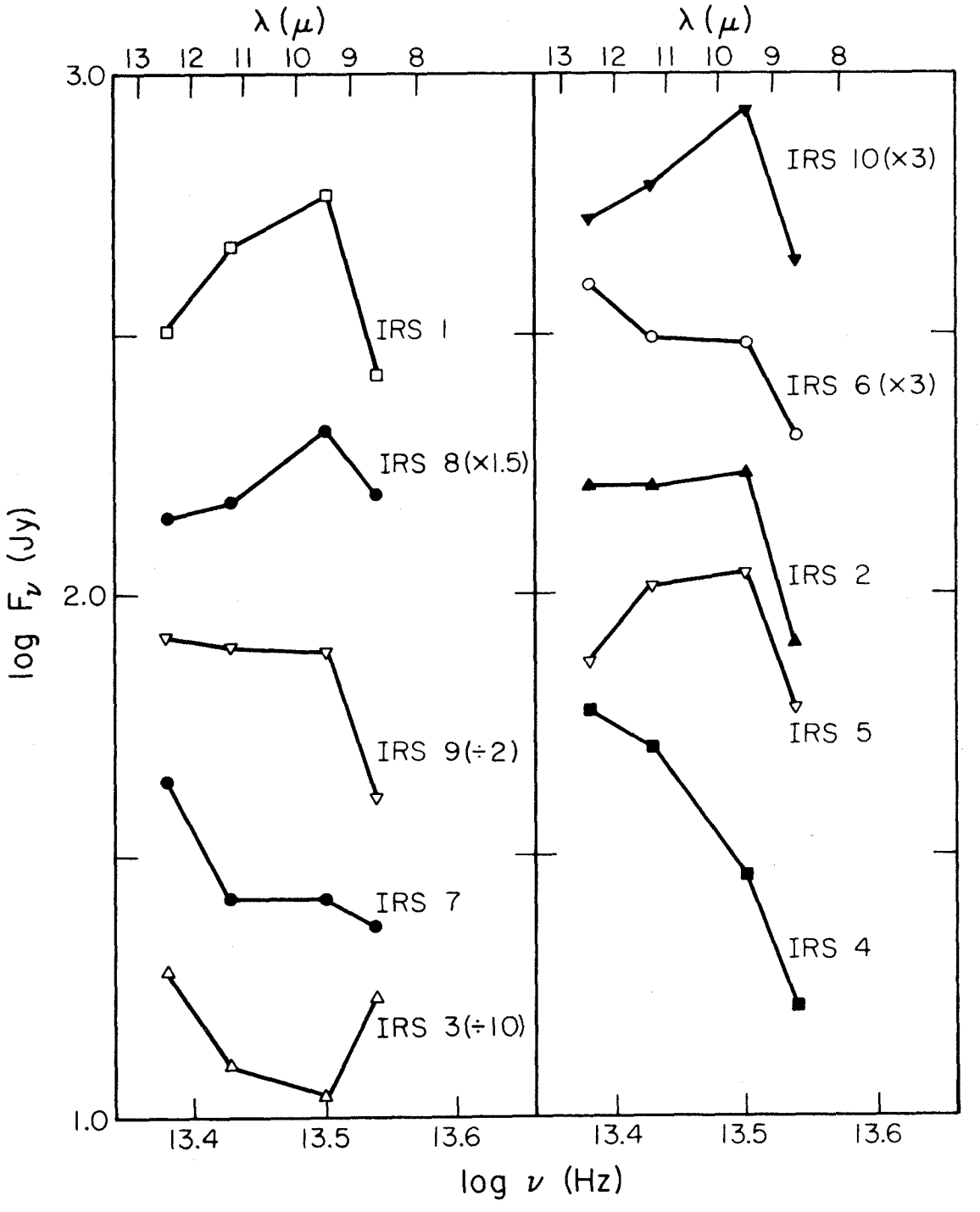

Figure 7

8 to 13-μ energy distributions corrected for extinction of all ten 10-μ sources observed.

of dust found by the above method is typically 10^4 for compact H II regions (Gillett et al. 1975); if this ratio holds, the total mass of a compact source is of order 1 $M_\odot$. This mass is to be compared with the total of 1 to 10 $M_\odot$ within a 5" aperture, derived from observations of the Ne line by assuming the abundance of Ne II is the same as the cosmic abundance of neon. The small mass derived for the compact sources provides further evidence that the density along the ridge is little affected by the compact sources. A lower limit to the luminosities of the sources can be computed from the corrected fluxes given in Figures 6 and 7, if it is assumed that the sources have a Rayleigh-Jeans energy distribution at wavelengths longer than the longest observed. The luminosities are of order 10^5 $L_\odot$; the largest, that of IRS1, is 4×10^5 $L_\odot$. These luminosities are typical of 06 or 07 main sequence stars (Panagia 1973), and one such star produces about enough ionizing photons to account for the Ne II emission in a 5" aperture. The compact sources along the ridge, if they are O stars, would be sufficient to ionize the ridge, but additional sources of high energy photons are necessary to maintain the ionization of the extended background discussed below.

Finally, the 10-μ sources are not all the same. IRS9 is relatively brighter at 2.2 μ than the other 10-μ sources and has a [1.6μ] - [2.2μ] color indicative of the presence of stars, as shown in Figure 6. IRS1 is also relatively bright at 2.2 μ.

f) Other Sources - IRS3 and 8

IRS3 is a unique source in the Galactic center complex because it is an isolated, unresolved source (BN) and has a larger silicate absorption than any other source (Table 3). Also, as shown in Figure 6, the spectrum at wavelengths of 5 μ and longer is bluer than that of IRS1 and 9. In fact, the energy distribution of IRS3 most closely resembles those of the Becklin-Neugebauer object in Orion (Becklin, Neugebauer, and Wynn-Williams 1973), or 1612 MHz OH sources studied by Beckwith and Evans (1976), all of which have silicate absorptions and higher color temperatures than the ridge sources.

The nature of IRS8 is unknown. Because it is isolated, IRS8 is easier to study than the ridge sources. Its high color temperature would suggest that it is like IRS3, and no Ne II was detected from it. The Ne II upper limit is, however, twice the equivalent width observed in the ridge sources and is therefore not significant. As shown in Figure 6, IRS8 has no silicate absorption; it has been spatially resolved (BN). Pending detection of Ne II or a significant upper limit, it appears that IRS8 is a source similar to those along the ridge. If so, its isolation from other sources makes it unlikely that all the ionizing radiation comes from a central source.

g) Extended Emission - IRS4

Approximately one-fourth of the 10-μ flux from the region mapped by BN is due to low surface brightness extended emission. This emission

shows up in the present results as a difference in the flux as measured with the spectrometer using a 5" aperture from that measured with broadband filters using a 2".3 aperture. The difference is largest at the longest wavelength, 12.5 μ, indicating that the background is very red. Furthermore, for IRS4, the reddest source near 10 μ, the difference is the same at all wavelengths. If a source with the color of IRS4, an intensity of about 10^{-16} W m^{-2} Hz^{-1} $ster^{-1}$, and a size larger than the 5" beam is subtracted from the spectrometer observations, the spectrometer colors agree very well with the broadband colors. It therefore appears that the extended background is similar in color to IRS4; in fact IRS4, which is itself very extended, may be merely a condensation in the extended background.

Most of the Ne II flux observed by Aitken et al. (1976) in a 25" aperture must come from the extended background. This can be seen by comparing the sum of all the Ne II fluxes given in Table 4 to the total flux. A few of the discrete sources were not observed with the spectrometer and so are not included in Table 4, but the observations in Table 4 all include some contribution from the extended background. The equivalent width of the Ne II line in a 25" aperture is 0.035 μ (Aitken et al. 1976), the same as that of the Ne II line in IRS4. This strengthens the conclusion that the spectra are similar.

That there is Ne II flux from the extended background was shown more directly by Wollman et al. (1976), who detected emission from regions where there are no discrete sources. Their observations show that emission comes from a region at least one arc minute in

diameter. It seems likely that this emission region coincides with the northern far-infrared source in the map of Harvey, Campbell, and Hoffmann (1976). It would be interesting to see if there is any Ne II emission from their southern source.

IV. CONCLUSIONS

The main conclusions of this study are as follows: (1) IRS7, 11, 12, 16, and 19, the sources with the bluest energy distributions between 1.6 and 3.5 μ, are stars or star clusters. The luminosity of IRS7 is about 10^5 $L_\odot$, while the other sources have luminosities of order 10^4 $L_\odot$. IRS7 has excess emission near 10 μ. (2) There is extended emission from ionized gas and dust. The emission peaks at the ridge, where the dust temperature is higher than average, and on IRS4. (3) The density of ionized gas in the discrete sources along the ridge is no higher than elsewhere on the ridge. The ridge consists of an H II region, which is density bounded. (4) IRS3 is a compact source, not associated with the ridge, of unknown nature. IRS8 may be similar to the compact sources along the ridge, or may also be unique. (5) The extinction is moderately uniform towards most of the sources observed. The visual extinction is about 28 magnitudes, and the 9.7-μ extinction is about 3.7 magnitudes.

REFERENCES

Aitken, D. K., Griffiths, J., Jones, B., and Penman, J. M. 1976, in press.

Aitken, D. K., Jones, B., and Penman, J. M. 1974, M.N.R.A.S., 169, 35P.

Balick, B. and Brown, R. L. 1974, Ap. J., 194, 265.

Becklin, E. E. and Neugebauer, G. 1968, Ap. J., 151, 145.

Becklin, E. E. and Neugebauer, G. 1975, Ap. J., 200, L71.

Becklin, E. E., Neugebauer, G., Wynn-Williams, C. G. 1973, Ap. J., 182, L7.

Beckwith, S. and Evans, N. J. 1976, in preparation.

Day, K. L., Steyer, T. R., and Huffman, D. R. 1974, Ap. J., 191,415.

Ekers, R. D., Goss, W. M., Schwarz, M. J., Downes, D., and Rogstad, D. 1975, Astron. and Ap., 43, 159.

Gehrz, R. D. 1972, Ap. J., 178, 715.

Gillett, F. C. and Forrest, W. J. 1973, Ap. J., 179, 483.

Gillett, F. C., Forrest, W. J., Merrill, K. M., Capps, R. W., and Soifer, B. T. 1975, Ap. J., 200, 609.

Hackwell, J. A., Gehrz, R. D., and Woolf, N. J. 1970, Nature, 227, 822.

Harvey, P. M., Campbell, M. F., and Hoffmann, W. F. 1976, in press.

Hoffmann, W. F., Frederick, C. L., and Emery, R. J. 1971, Ap. J., 164, L23.

Humphreys, R. M., and Ney, E. P. 1974, Ap. J., 194, 623.

Knacke, R. F. and Thomson, R. K. 1973, P.A.S.P., 85, 341.

Lo, K. Y., Schilizzi, R. T., Cohen, M. H., and Ross, H. N. 1975, Ap. J., 202, L63.

Low, F. J., Kleinmann, D. E., Forbes, F. F., and Aumann, H. H. 1969, Ap. J., 157, L97.

Neugebauer, G., Becklin, E. E., Beckwith, S., Matthews, K., and Wynn-Williams, C. G. 1976, Ap. J., in press.

Panagia, N. 1973, Astron. J., 78, 929.

Penman, J. M. 1976, in press.

Rieke, G. H. and Low, F. J. 1973, Ap. J., 184, 415.

Sandage, A. R., Becklin, E. E., and Neugebauer, G. 1969, Ap. J., 157, 55.

Willner, S. P. 1976, in preparation.

Wollman, E. R., Geballe, T. R., Lacy, J. H., and Townes, C. H. 1976, Ap. J., in press.